29. Hendricksen M, Thomas AJ, Ferrier IN, Ince P, O'Brien JT. Neuropathological study of the dorsal raphe nuclei in late-life depression and Alzheimer's disease with and without depression. *Am J Psychiatry.* 2004;161:1096–1102.
30. Ichimiya T, Suhara T, Sudo Y, et al. Serotonin transporter binding in patients with mood disorders: a PET study with [^{11}C](+)McN5652. *Biol Psychiatry.* 2002;51:715–722.
31. Li T, Holmes C, Sham PC, et al. Allelic functional variation of serotonin transporter expression is a susceptibility factor for late onset Alzheimer's disease. *Neuroreport.* 1997;8:683–686.
32. Aucoin JS, Jiang P, Aznavour N, et al. Selective cholinergic denervation, independent from oxidative stress, in a mouse model of Alzheimer's disease. *Neuroscience.* 2005;132:73–86.
33. Holthoff VA, Beuthien-Baumann B, Kalbe E, et al. Regional cerebral metabolism in early Alzheimer's disease with clinically significant apathy or depression. *Biol Psychiatry.* 2005;57:412–421.
34. Mayberg HS, Liotti M, Brannan SK, et al. Reciprocal limbic-cortical function and negative mood: converging PET findings in depression and normal sadness. *Am J Psychiatry.* 1999;156:675–682.
35. Kennedy SH, Evans KR, Krüger S, et al. Changes in regional brain glucose metabolism measured with positron emission tomography after paroxetine treatment of major depression. *Am J Psychiatry.* 2001;158:899–905.
36. Grafman J, Schwab K, Warden D, Pridgen A, Brown HR, Salazar AM. Frontal lobe injuries, violence, and aggression: a report of the Vietnam Head Injury Study. *Neurology.* 1996;46:1231–1238.
37. Eustache F, Piolino P, Giffard B, et al. 'In the course of time': a PET study of the cerebral substrates of autobiographical amnesia in Alzheimer's disease. *Brain.* 2004;127:1549–1560.
38. Mattson MP, Maudsley S, Martin B. BDNF and 5-HT: a dynamic duo in age-related neuronal plasticity and neurodegenerative disorders. *Trends Neurosci.* 2004;27:589–594.
39. Nelson RL, Guo Z, Halagappa VM, et al. Prophylactic treatment with paroxetine ameliorates behavioral deficits and retards the development of amyloid and tau pathologies in 3xTgAD mice. *Exp Neurol.* 2007;205:166–176.
40. Steele C, Rovner B, Chase GA, Folstein M. Psychiatric symptoms and nursing home placement of patients with Alzheimer's disease. *Am J Psychiatry.* 1990; 147:1049–1051.

International Psychogeriatrics (2009), 21:1, 148–156 © 2008 International Psychogeriatric Association
doi:10.1017/S1041610208008132 Printed in the United Kingdom

Decreased cortical glucose metabolism in converters from CDR 0.5 to Alzheimer's disease in a community: the Osaki-Tajiri Project

Hiroshi Ishii,[1,2] Hiroyasu Ishikawa,[1,3] Kenichi Meguro,[1,3] Manabu Tashiro[4] and Satoshi Yamaguchi[1,3]

[1] *Department of Geriatric Behavioral Neurology, Tohoku University Graduate School of Medicine, Sendai, Japan*
[2] *Kawasaki Kokoro Hospital, Kawasaki, Japan*
[3] *The Osaki-Tajiri SKIP Center, Osaki, Japan*
[4] *Division of Nuclear Medicine, Cyclotron Radioisotope Center, Tohoku University, Sendai, Japan*

ABSTRACT

Background: Several follow-up [^{18}F]fluorodeoxy glucose (FDG)-positron emission tomography (PET) studies have been performed in patients with mild cognitive impairment, but none have examined subjects with a Clinical Dementia Rating (CDR) of 0.5. Therefore, we used FDG-PET to investigate whether baseline glucose metabolism (CMRglc) in CDR 0.5 converters to dementia showed changes consistent with early Alzheimer's disease (AD).

Methods: Based on our earlier study, which we refer to as Prevalence Study 1998, we were able to examine 14 CDR 0, 42 CDR 0.5, and 12 AD subjects with PET and follow these subjects for five years. Baseline neuropsychological and CMRglc values were compared among groups of CDR 0, CDR 0.5/converters, CDR 0.5/non-converters, and AD subjects.

Results: All CDR 0 subjects were reassessed as CDR 0 after the five-year period. For CDR 0.5 subjects, 20 had converted to AD and 22 remained as CDR 0.5. In cognitive tests, CDR 0.5/converters showed significantly deteriorated recent memory function compared with CDR 0.5/non-converters at the baseline evaluation. Most brain areas showed decreased CMRglc in AD patients. CDR 0.5/converters had a significantly lower baseline CMRglc in the right cingulate, left inferior parietal and left temporal gyrus compared with CDR 0.5/non-converters.

Conclusions: Our findings suggest that CDR 0.5/converters have a baseline metabolic decline in areas that might be specific to AD.

Key words: MCI, CDR 0.5, FDG, PET, Alzheimer's disease

Introduction

Early diagnosis of the borderline condition between healthy aging and dementia may be important for health policy planning for dementia prevention or early intervention, since some borderline cases are reported to be reversible (Larrieu *et al.*, 2002). This condition is referred to as mild cognitive impairment (MCI) (Petersen *et al.*, 1997) or Clinical Dementia Rating (CDR; Morris, 1993) 0.5, and the rate of progression to dementia is 8–20% per year. Impairment of cognitive functions such as recent memory and executive function (Chen *et al.*, 2000) and a lower clinical observation score (Morris *et al.*, 2001) are predictors of decline.

Hippocampal atrophy (Visser *et al.*, 2002) shown by magnetic resonance imaging (MRI) is characteristic of the neurological background of CDR 0.5 subjects, particularly in association with early Alzheimer's disease (AD). Five major longitudinal studies of MCI have been performed using the baseline cerebral metabolic rate for glucose (CMRglc) determined by positron emission tomography (PET) with [^{18}F]fluoro-deoxyglucose (FDG) (Arnaiz *et al.*, 2001; Chetelat *et al.*, 2003; Drzezga *et al.*, 2003; Mosconi *et al.*, 2004; Fellgiebel *et al.*, 2007). All these studies used clinic samples, with four using neuropsychological tests based on Petersen's MCI criteria (Petersen *et al.*, 1997) and the fifth using Global Deterioration Scale (GDS)

Correspondence should be addressed to: Kenichi Meguro, MD, PhD, Department of Geriatric Behavioral Neurology, Tohoku University Graduate School of Medicine, 2-1, Seiryo-machi, Aoba-ku, Sendai 980-8575, Japan. Email: k-meg@umin.ac.jp. Received 19 May 2008; revision requested 28 Jul 2008; revised version received 17 Sep 2008; accepted 25 Sep 2008. First published online 1 December 2008.

3 criteria (Reisberg *et al.*, 1982). After following the subjects for 1–3 years, amnestic MCI subjects showing AD-like metabolic changes (decreased CMRglc in the temporoparietal areas and posterior cingulate) were found to be at risk for conversion to AD.

Follow-up FDG-PET has not been performed in CDR 0.5 subjects, but follow-up with other approaches has indicated that CDR 0.5 subjects with a higher CDR-sum of boxes (SB) score more frequently decline to AD compared with those with lower CDR-SB scores (Morris *et al.*, 2001). CDR 0.5 subjects with a higher SB score also show decreased metabolism in AD-specific areas (Perneczky *et al.*, 2007). These results suggest that CDR 0.5 converters to AD have an AD-like metabolic pattern, and the aim of this study was to examine this hypothesis using FDG-PET in our MCI/CDR 0.5 cohort.

The Osaki-Tajiri Project, previously called the Tajiri Project, is a community-based program on stroke, dementia, and bed-confinement prevention in Osaki, northern Japan. In our Prevalence Study 1998 (Meguro *et al.*, 2002), we reported rates of CDR 0.5 and MCI of 30.1% and 4.9%, respectively, with CDR 0.5 having a significantly greater prevalence (Meguro *et al.*, 2004). Among the participants in Prevalence Study 1998, we were able to examine CMRglc for 68 people and follow them for five years, after which we examined the incidence of dementia that developed in CDR 0 and 0.5 subjects (Incidence Study 2003; Meguro *et al.*, 2007). In the current study, we investigated whether the baseline CMRglc of CDR 0.5 converters to dementia manifests as metabolic changes specific to early AD.

Methods

Participants

In Prevalence Study 1998, 564 adults from among an epidemiologic population of 1,654 were randomly selected to undergo MRI (1.5T, Shimazu, Japan). The cost of all the MRIs was officially borne by the town. Finally, 497 participants agreed to undergo MRI: 346 CDR 0 (healthy), 119 CDR 0.5 (questionable dementia), and 32 CDR 1+ (dementia) subjects. T1-weighted (TR/TE 400/14) and T2-weighted (TR/TE 3000/90) images were used for assessing atrophy and cerebrovascular diseases, as described previously (Meguro *et al.*, 2002).

Owing to the limited time available for FDG-PET examination at Tohoku University Cyclotron Radioisotope Center (an average of four patients a month), we had to select subjects who would receive PET. From the 497 subjects who underwent MRI, we randomly selected 35 CDR 0 (10% of 346) and 60 CDR 0.5 (50% of 119) subjects, and all 14 AD patients among the CDR 1+ group, for PET. Finally, we were able to examine 68 subjects using PET: 14 CDR 0, 42 CDR 0.5, and 12 AD. The other subjects refused to undergo PET examinations due to "psychological" reasons and the travelling distance between the community and the PET center (a one-hour drive).

All AD patients had a rating of CDR 1 and met the NINCDS-ADRDA criteria for probable AD (McKhann *et al.*, 1984). All CDR 0.5 subjects showed mild cognitive dysfunction, but this did not affect their daily lives in the community and none met the DSM-IV criteria for dementia (American Psychiatric Association, 1994). All 68 subjects met the following inclusion criteria: (1) no history of stroke, head injury or systemic disorders that could affect brain function, and normal values of vitamin B_1, B_6, B_{12}, folate, and thyroid hormones; (2) no cerebrovascular diseases as shown by MRI, and no marked neurological signs and symptoms; and (3) agreement of the subjects and family members to participate in Incidence Study 2003 and to be followed for five years.

Written informed consent was obtained from all CDR 0 and 0.5 subjects and from the families of CDR 0.5 and AD patients. The study was approved by the Ethical Committee of the Cyclotron Radioisotope Center of Tohoku University and the Tajiri SKIP Center.

CDR assessment

A clinical team of doctors and public health nurses determined the CDR while blinded to the cognitive tests (see below) and PET findings. Before being interviewed by the doctors, public health nurses visited the participants' homes to evaluate their daily activities. Observations by family members regarding the participants' lives were described in a semi-structured questionnaire; for participants who lived alone, public health nurses visited them frequently to evaluate their daily lives. The participants were interviewed by doctors to assess episodic memory, orientation, problem solving and judgment. Finally, the CDR stages were decided at a joint meeting, with reference to the information provided by the family. A reliable Japanese version of the CDR Work Sheet (Meguro, 2004) has been established, and one of the authors (K.M) has been certified as a CDR rater at the Alzheimer's Disease Research Center, Washington University School of Medicine. CDR 0.5 participants who converted to AD were classified as CDR 0.5/converters and those who did not convert as CDR 0.5/non-converters.

The CDR was evaluated using the same approach at baseline and follow-up.

Cognitive assessment

A team of trained psychologists performed cognitive tests while blinded to the CDR stages and PET findings. These tests included the Mini-mental State Examination (MMSE; Folstein *et al.*, 1975) and the Cognitive Abilities Screening Instrument (CASI) (Teng *et al.*, 1994). The CASI has nine domains: long-term memory, short-term memory, attention, concentration/mental manipulation, orientation, visual construction, abstraction and judgment, list-generating fluency, and language. The long-term memory domain evaluates knowledge and remote memory, and herein we refer to this domain as "remote memory." The short-term memory domain assesses delayed recall of three words presented orally and immediate recall of five objects presented visually, and we refer to this domain as "recent memory."

PET

The PET study was performed with a model PT931/04-12 scanner (CTI Inc., USA; axial/transaxial resolutions: 8 mm) using [^{18}F]fluoro-deoxyglucose (FDG) (Phelps *et al.*, 1979; Reivich *et al.*, 1979). A short cannula was placed in a radial artery for blood sampling. Each subject was positioned with the OM line parallel to the detector rings according to brain slices collected by MRI. A cross of light was projected onto marks on the subject's head, which were set at standard points of 30 mm and 77 mm above and parallel to the OM line. A 20-minute transmission scan was performed using a ^{68}Ge/^{68}Ga external ring source. Thirty to 45 minutes after injection of 5–12 mCi of FDG, two emission scans were performed and data were collected simultaneously from each of seven contiguous axial sections. A total of 14 slices parallel to the OM line with a thickness of 6 mm were analyzed, encompassing virtually the whole brain. The detailed methodology has been described previously (Yamaguchi *et al.*, 1997).

Imaging analyses

ROI

After two different pairs of axial T1-weighted MRI and PET images were matched with each other at the same brain slice, the position of the regions of interest (circular ROIs, 2.7 cm^2) were defined manually using the overlapped images. A total of 13 ROIs in each hemisphere were selected: upper frontal, anterior frontal, inferior frontal, parietal, temporo-parieto-occipital, primary auditory, temporal, hippocampus, primary visual, occipital, basal ganglia, cerebellum, and white matter. The detailed methodology has been described previously (Yamaguchi *et al.*, 1997).

SPM

Basic image processing and voxel-based data analysis were performed using SPM2 (Wellcome Department of Cognitive Neurology, London, U.K.) on a Windows XP machine. PET data were subjected to an affine and non-linear spatial normalization into the standard MNI PET template of SPM2, and to re-slicing of 2×2×2 mm. The PET images were smoothed using an isotropic Gaussian filter of 12 mm in diameter to compensate for intersubject gyral variability and to reduce high-frequency noise. The anatomically standardized images were then normalized by ANCOVA to a mean value of 50 mg/100 g/min. The four groups (CDR 0, CDR 0.5/non-converters, CDR 0.5/converters, AD) were compared with ANCOVA (covariance of age and educational level). Pairs of groups were compared with unpaired t-tests. For multiple comparison, significance was accepted if the voxels survived an uncorrected threshold of $p<0.001$.

Individual analysis

Individual CMRglc pattern analysis was conducted using the classification of Silverman *et al.* (2001): N1, normal metabolism; N2, global hypometabolism; N3, focal hypometabolism; P1, parietal/temporal with/without frontal hypometabolism; P2, frontal predominant hypometabolism; P3, hypometabolism of both the caudate head and lentiform nuclei. N indicates non-progressive PET patterns, and P shows progressive PET patterns. P1 indicates a PET pattern consistent with AD, and P2 and P3 indicate progressive but non-AD patterns. The patterns were compared between CDR 0.5/non-converters and CDR 0.5/converters by χ^2 test.

Clinical reassessments

In Incidence Study 2003, the CDR stages of all the subjects in the current PET study were reassessed to determine whether they met the criteria for dementia and AD. The reassessments were performed by evaluators who were blinded to the baseline CDR, neuropsychological tests, and PET findings. We mainly focused on CDR 0.5 subjects to determine whether they met the criteria for CDR 1 and AD.

Results

Clinical outcome

All participants in the CDR 0 group were reassessed as CDR 0 after the five-year period. In the CDR 0.5 group, 20 participants converted to AD (CDR 0.5/converters) and 22 participants remained as CDR 0.5 (CDR 0.5/non-converters). All AD patients declined to CDR 2. The demographics of the four groups are shown in Table 1. Age and educational level did not differ significantly among the groups. The AD group had significantly lower cognitive scores compared with the other groups.

Cognitive impairment

The CASI scores of the four groups are shown in Table 2. The AD group had significantly lower scores for all domains except "remote memory," compared with the other groups. CDR 0.5/converters showed a significantly lower "recent memory" score compared with CDR 0.5/non-converters.

Baseline glucose metabolism

Absolute rCMRglc values were calculated using arterial blood sampling and autoradiography. Using the ROI method, we found that the AD group had severely decreased rCMRglc compared with other groups, except in the basal ganglia and white matter, as shown in Table 3. There was no significant difference between CDR 0.5/non-converters and the CDR 0 group. However, CDR 0.5/converters had decreased rCMRglc in the temporoparieto-occipital (TPO) and hippocampus compared with CDR 0 subjects, and decreased rCMRglc in the TPO compared with CDR 0.5/non-converters.

SPM

Comparisons of CDR 0.5 subjects with CDR 0 subjects and AD patients

Comparisons of CDR 0.5/converters and CDR 0.5/non-converters with CDR 0 subjects are shown in Figure 1, and similar comparisons with AD

Table 1. Demographics of the study population at baseline

GROUP	MALE/FEMALE	AGE (y)	EDUCATION (y)	CASI TOTAL
CDR 0	4/10	77.7 (1.5)	8.4 (0.2)	89.7 (1.4)
CDR 0.5/non-converters	7/15	78.0 (1.6)	8.4 (0.2)	87.9 (1.6)
CDR 0.5/converters	7/13	78.4 (1.7)	9.1 (0.3)	79.9 (1.7)
AD	6/6	80.0 (1.8)	8.3 (0.4)	50.7 (2.4)†

Shown are the mean (SD).
Age (one-way ANOVA, F = 2.410, p = 0.081) and educational level (F = 0.393, p = 0.0759) did not differ significantly among the groups. The AD group had significantly lower cognitive scores compared with the other groups (F = 35.810, p<0.0001)(†).
CDR = Clinical Dementia Rating, AD = Alzheimer's disease.
CASI = Cognitive Abilities Screening Instrument.

Table 2. Cognitive performances of four groups at baseline

CASI ITEMS	CDR 0	CDR 0.5/ NON-CONVERTERS	CDR 0.5/ CONVERTERS	AD	F VALUE	p VALUE
Remote Memory	10.0 (0.0)	10.0 (0.0)	9.6 (0.8)	8.3 (2.9)	2.209	0.073
Recent Memory	10.8 (1.6)	10.8 (1.6)	6.8 (3.1)[a,b]	2.8 (1.9)[a,b,c]	20.900	0.000
Attention	6.5 (1.3)	6.8 (1.7)	6.9 (1.0)	4.4 (2.0)[b,c]	3.860	0.006
Concentration/ Mental Manipulation	7.3 (1.7)	7.6 (1.6)	7.5 (2.0)	3.8 (3.4)[a,b,c]	6.402	0.000
Orientation	17.8 (0.4)	16.7 (3.1)	15.2 (3.3)	5.3 (3.7)[a,b,c]	26.056	0.000
Visual Construction	9.9 (0.3)	9.7 (0.7)	9.7 (0.5)	7.7 (2.4)[a,b,c]	5.880	0.000
Abstraction and Judgement	9.2 (2.2)	8.8 (2.1)	6.9 (2.0)	5.1 (2.9)[a,b]	5.886	0.000
List-generating Fluency	8.0 (1.8)	7.6 (2.2)	6.5 (1.8)	4.3 (2.0)[a,b]	6.159	0.000
Language	9.8 (0.4)	9.9 (0.3)	9.7 (0.5)	8.2 (2.0)[a,b]	4.057	0.005

Showns are the mean (SD).
ANCOVA among four groups with the age and education level as covariance was performed.
The AD group had significantly lower scores for all domains except "remote memory," compared with the other groups (ANCOVA, covariance of age and educational level, p = 0.008). CDR 0.5/converters showed a significantly lower "recent memory" score compared with CDR 0.5/non-converters (ANCOVA, covariance of age and educational level, p = 0.008). post hoc tests, significantly (p<0.05) different from Normal (a), CDR 0.5/non-converters (b), and CDR 0.5/converters (c).
CDR = Clinical Dementia Rating, AD = Alzheimer's disease.

Table 3. ROI values of four groups

ROI	CDR 0 NORMAL (n = 14)	CDR 0.5/NON-CONVERTERS (n = 22)	CDR 0.5/ CONVERTERS (n = 20)	CDR 1+AD (N = 12)	MS	F-VALUE	p-VALUE
Upper frontal	8.58 (1.17)	8.31 (0.43)	8.13 (0.38)	5.73 (0.86)[abc]	22.433	44.054	<0.001
Anterior frontal	7.64 (1.33)	7.09 (0.49)	6.90 (0.63)	4.64 (1.03)[abc]	22.522	30.436	<0.001
Inferior frontal	6.72 (1.31)	6.24 (0.51)	6.08 (0.42)	4.96 (0.90)[abc]	7.061	11.258	<0.001
Parietal	8.35 (1.13)	8.02 (0.42)	7.99 (0.47)	5.46 (0.83)[abc]	23.181	46.317	<0.001
TPO	7.31 (1.13)	6.87 (0.36)	5.84 (0.43)[ab]	4.34 (1.07)[abc]	23.774	43.005	<0.001
Primary auditory	8.81 (0.85)	8.59 (0.44)	8.54 (0.44)	5.16 (0.96)[abc]	39.814	93.525	<0.001
Temporal	6.89 (1.35)	6.42 (0.48)	6.26 (0.53)	4.50 (0.93)[abc]	14.053	20.761	<0.001
Hippocampus	6.20 (0.86)	6.05 (0.52)	5.45 (0.70)[a]	4.50 (0.95)[abc]	8.106	15.092	<0.001
Primary visual	9.34 (1.24)	8.43 (0.51)	8.19 (0.63)	5.70 (0.84)[abc]	29.721	24.293	<0.001
Occipital	7.91 (1.18)	7.11 (0.50)	6.54 (0.91)	4.16 (0.82)[abc]	42.626	52.311	<0.001
Basal ganglia	6.58 (1.16)	6.43 (0.27)	6.38 (0.30)	6.02 (0.76)	0.723	1.716	0.172
Cerebellum	7.32 (1.20)	7.39 (0.31)	7.27 (0.43)	6.06 (1.00)[abc]	5.371	9.721	<0.001
White matter	5.94 (1.08)	5.70 (0.32)	5.62 (0.52)	5.38 (0.88)	0.701	1.458	0.234

Shown are the means (SD).
The AD group had severely decreased rCMRglc compared with other groups, except in the basal ganglia and white matter (multiple ANOVAs and post hoc tests). There were no significant differences between CDR 0.5/non-converters and the CDR 0 group. However, CDR 0.5/Converters had decreased rCMRglc in the TPO and hippocampus compared with CDR 0 subjects, and decreased rCMRglc in the TPO compared with CDR 0.5/non-converters.
post hoc tests, significantly ($p<0.05$) different from Normal (a), CDR 0.5/non-converters (b), and CDR 0.5/converters (c).
ROI = region of interests, TPO = Temporo-parieto-occipital, CDR = Clinical Dementia Rating, con. = converters, AD = Alzheimer's disease.

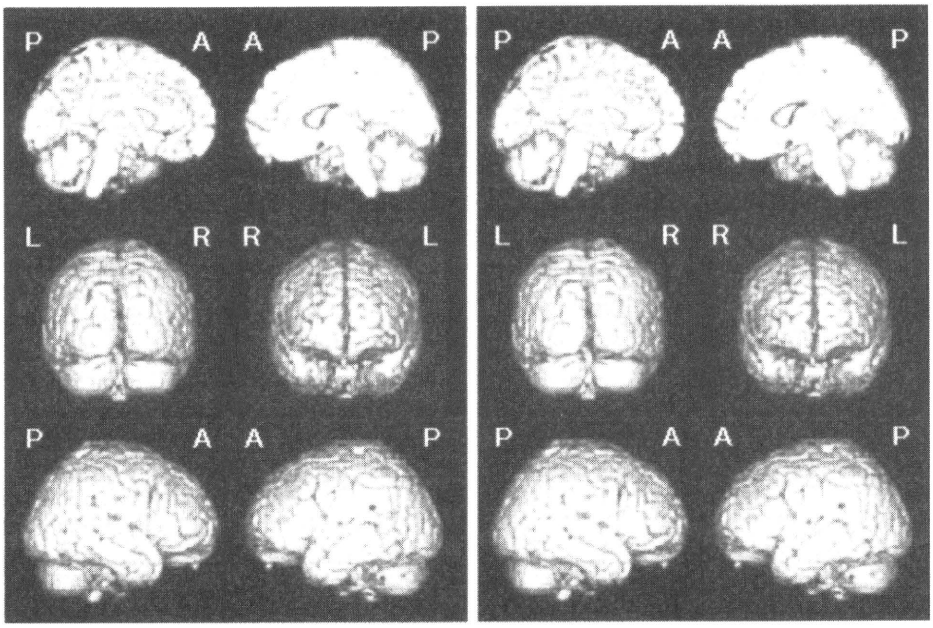

(a) CDR 0.5/Converters < CDR 0 (b) CDR 0.5/Non-converters < CDR 0

Figure 1. Results from voxel-based analysis with SPM2. (a) Voxels showing significant hypometabolism for CDR 0.5/converters compared to CDR 0 subjects ($p<0.001$, uncorrected). (b) Voxels showing significant hypometabolism for CDR 0.5/non-converters compared to CDR 0 subjects ($p<0.001$, uncorrected). The local maxima for the brain regions are shown in Table 3.

patients are shown in Figure 2. A region of hypometabolism was considered significant at $p<0.001$ (uncorrected) for a cluster of ≥ 20 contiguous voxels superimposed on 3D-rendered MR images in Montreal Neurological Institute (MNI) space (Evans *et al.*, 1994). Brain areas reaching the significance threshold were identified by voxel coordinates and labeled according to Talairach and Trournoux after coordinate conversion from MNI to Talairach space using a non-linear transformation algorithm (http://imaging.mrc-cbu.cam.ac.uk/imaging/MniTalairach) (Talairach and Trournoux,

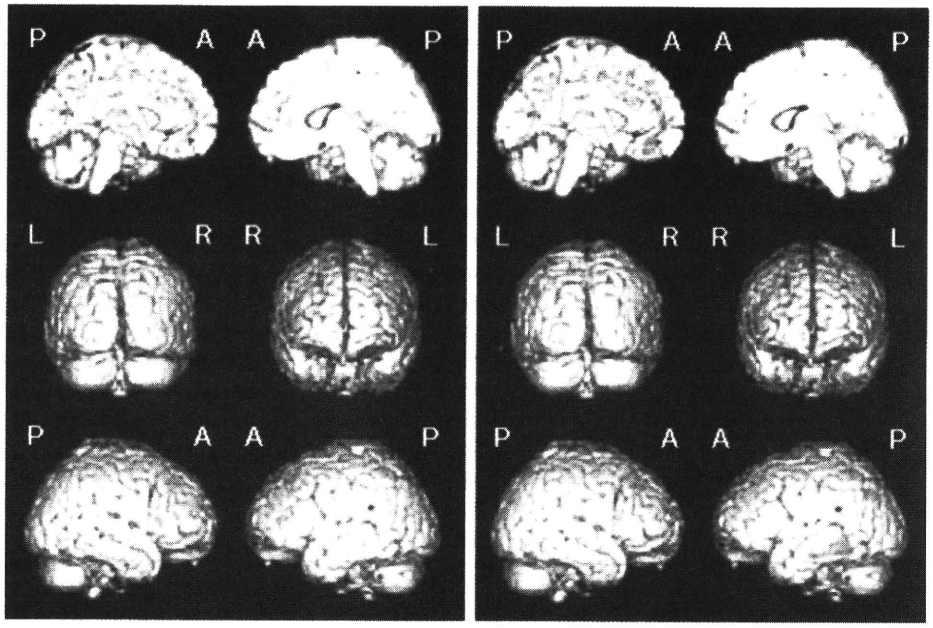

(a) AD < CDR 0.5/Converters (b) AD < CDR 0.5/Non-converters

Figure 2. (a) Voxels showing significant hypometabolism for patients with AD compared to CDR 0.5/converters ($p<0.001$, uncorrected). (b) Voxels showing significant hypometabolism for patients with AD compared to CDR 0.5/non-converters ($p<0.001$, uncorrected).

Table 4. Location and peak coordinates of significant voxels from voxel-based analysis using SMP2

TALAIRACH COORDINATES					
x	y	z	T STATISTICS	BRODMANN	ANATOMIC REGION
CDR 0.5/converters < CDR 0					
−44	−53	19	4.04	22	Left superior temporal gyrus
−44	−46	17	3.57	22	Left superior temporal gyrus
36	−36	−13	4.01	36	Right parahippocampal gyrus
CDR 0.5/con-converters < CDR 0					
8	51	20	3.59	9	Right medial frontal gyrus
AD < CDR 0.5/converters					
44	20	10	4.04	45	Right inferior frontal gyrus
AD < CDR 0.5/non-converters					
−55	−45	−8	4.91	21	Left middle temporal gyrus
−57	−32	−15	3.77	20	Left inferior Temporal gyrus
−26	−45	−8	4.14	37	Left fusiform gyrus
46	18	10	4.08	45	Right inferior frontal gyrus
−10	57	5	3.97	10	Left medial frontal gyrus
−12	38	−20	3.70	11	Left straight gyrus
−5	34	−8	3.54	32	Left cingulate gyrus
−44	−71	35	3.37	39	Left angular gyrus
CDR 0.5/converters < CDR 0.5/non-converters					
−40	−61	25	3.85	39	Left middle temporal gyrus
−46	−40	22	3.61	40	Left inferior parietal lobule
12	−37	37	3.61	31	Right cingulate gyrus
−55	−43	−11	3.51	37	Left inferior temporal gyrus

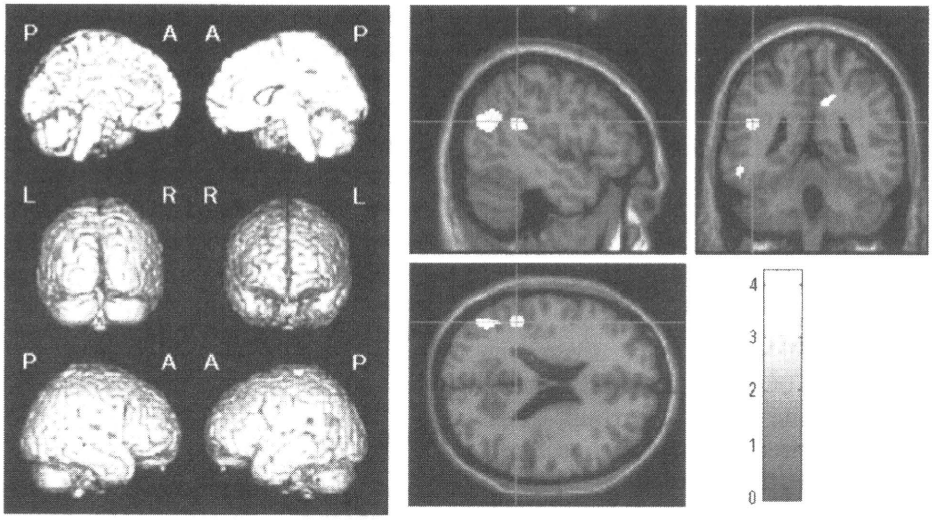

Figure 3. (Left) Voxels showing significant hypometabolism for CDR 0.5/converters compared to CDR 0.5/non-converters ($p<0.001$, uncorrected). (Right) The same results were displayed on 2D planes of a normal MRI template provided by SPM2 to clarify their anatomic locations. The color bar represents t values derived from the voxel-based analysis.

Table 5. PET patterns of Silverman's classification for two CDR 0.5 groups

	N1	N2	N3	P1	P2	P3	TOTAL
Non-converters	5	5	7	5	0	0	23
Converters	3	1	4	12	0	0	20

N = non-progressive patterns, p = progressive patterns

1998). Areas showing a significant difference (SPM2, $p<0.001$, uncorrected) are shown in Table 4. For multiple comparisons, the significance level was set at 0.001.

COMPARISON BETWEEN CDR 0.5/CONVERTERS AND CDR 0.5/NON-CONVERTERS

CDR 0.5/converters had significantly lower CMRglc values (SPM2, $p<0.001$, uncorrected) in the left middle temporal gyrus, left inferior parietal lobule, right cingulate gyrus, and left inferior temporal gyrus, compared with CDR 0.5/non-converters (Figure 3 and see Table 4).

INDIVIDUAL ANALYSIS USING SILVERMAN'S CLASSIFICATION

PET patterns using Silverman's classification for the two CDR 0.5 groups are shown in Table 5. The difference between the groups was significant by χ^2 test ($p<0.05$), with CDR 0.5/converters showing a P1 pattern more frequently. No participants showed P2 or P3 patterns. Comparing all non-progressive patterns (N1–N3) with the progressive pattern (P1) for the two groups, a true positive rate (sensitivity) of 0.60, a true negative rate (specificity) of 0.74, a positive predictive value of 0.71, and a negative predictive value of 0.68 were found. Of the 14 normal subjects, 12 showed an N1 pattern and 2 had an N2 pattern. The 12 AD patients all showed P1 patterns.

Discussion

In this study, CDR 0.5/converters showed greater baseline hypometabolism compared with CDR 0.5/non-converters in brain areas specific for AD, suggesting that CDR 0.5 converters might have AD-like changes.

Methodological issues

There are some methodological limitations in the study. First, only 40% of the CDR 0 subjects and 70% of the CDR 0.5 subjects were scanned due to limited availability of the FDG-PET scanner (an average of four patients a month). The long distance between Tajiri and the PET center also prevented some older adults from participating in the study. Therefore, there may be some sampling bias and caution is required in interpretation of the results. Second, evaluation was only performed at two time points, rather than annually; however, the administrative situation brought about by the formation of a new city in 2006 through the merger of several towns, including Tajiri, prevented use of an annual study design. Third, although the CASI provided sufficient information for a detailed analysis, assessments such as the WMS-R for memory and the WAIS-R for general intelligence would have provided more cognitive information; however, the time required for assessing community residents prevented use of these tests.

Neuropsychological findings

Only the CASI "recent memory" score showed a significant difference between CDR 0.5/converters and CDR 0.5/non-converters ($p = 0.008$). This is consistent with previous studies (Arnaiz *et al.*, 2001; Visser *et al.*, 2002) and suggests that CDR 0.5/converters already have AD-like changes, since recent memory impairment is a well-known neuropsychological feature of AD.

Criteria for amnestic MCI

We evaluated the effect of amnestic MCI criteria retrospectively. Among the CDR 0.5 group, those who met the following criteria were also considered to have amnestic MCI (Meguro *et al.*, 2004): memory complaints, a CASI "recent memory" score of −1.5 SD lower than the normal values for each age group, and normal MMSE scores for each educational level. Four CDR 0.5 subjects met these criteria and all converted to AD. Although the sample size was small, these results suggest that criteria for amnestic MCI are more "specific" for AD changes, whereas CDR 0.5 criteria are more "sensitive."

Metabolic patterns of CDR 0.5 converters

The lack of metabolic differences after taking CASI scores into covariance might indicate that cognitive, rather than metabolic, differences predict conversion to AD. However, the aim of this study was to investigate whether metabolic changes in CDR 0.5 converters manifest as a decrease in CMRglc in a manner specific to early AD. Although the predictive power may be stronger for cognitive dysfunction, we believe that the findings support the hypothesis of the study.

Our findings suggest that CDR 0.5 participants who decline to AD develop hypometabolism in the posterior cingulate and other brain regions that might be specific to AD. These hypometabolic areas are similar to those observed in patients with probable AD (Hoffman *et al.*, 2000). Previous longitudinal studies on amnestic MCI have also indicated that these areas differ significantly between converters and non-converters (Arnaiz *et al.*, 2001; Chetelat *et al.*, 2003; Drzezga *et al.*, 2003; Mosconi *et al.*, 2004). A follow-up SPECT study on amnestic MCI also showed asymmetric reduction of perfusion in the parahippocampus, lateral parietal lobe, and posterior cingulate cortices in converters (Ishiwata *et al.*, 2006). Parahippocampal gyri are very small areas and other studies may have missed these regions using the SPM method.

Since SPM reveals much more restricted abnormalities than suggested by individual classification, analysis of the individual patterns is required to provide support for SPM findings. In individual analysis of the CMRglc pattern, the AD pattern (P1) was most frequent among CDR 0.5/converters, whereas N1 and N3 patterns were frequent in CDR 0.5/non-converters (Table 5). These results are consistent with past studies and indicate that most CDR 0.5/converters already have AD pathology. The data also support the results of SPM analysis, indicating that both visual and automated methods are preferable to confirm the reliability of acquired data.

Conclusion

Neurological findings for MCI/CDR 0.5 decliners may show manifestation of hypometabolism in brain areas specific to AD. Since the prevalence of CDR 0.5 is much higher than that of MCI and the rate of decline to dementia from the two conditions is about the same, use of CDR 0.5 criteria may increase the detection rate of decliners in a community population.

Conflict of interest

None.

Description of authors' roles

K. Meguro and H. Ishii designed the study, supervised the data collection and wrote the paper. K. Meguro and S. Yamaguchi collected the data. H. Ishikawa and M. Tashiro were responsible for the statistical design of the study and for statistical analysis.

Acknowledgments

We are grateful to the town officials of Tajiri. This study was supported in part by a JST grant for research and education in molecular imaging.

References

American Psychiatric Association (1994). *Diagnostic and Statistical Manual of Mental Disorders*, 4th edn. Washington, DC: American Psychiatric Association.

Arnaiz, E. *et al.* (2001). Impaired cerebral glucose metabolism and cognitive functioning predict deterioration in mild cognitive impairment. *NeuroReport*, 12, 851–855.

Chen, P., Ratcliff, G., Belle, S. H., Cauley, J. A., DeKosky, S. T., and Ganguli, M. (2000). Cognitive tests that best discriminate between presymptomatic AD and

those who remain nondemented. *Neurology*, 55, 1847–1853.

Chetelat, G., Desgranges, B., de la Sayette, V., Viader, F., Eustache, F. and Baron, J. C. (2003). Mild cognitive impairment: can FDG-PET predict who is to rapidly convert to Alzheimer's disease? *Neurology*, 60, 1374–1377.

Drzezga, A. *et al.* (2003). Cerebral metabolic changes accompanying conversion of mild cognitive impairment into Alzheimer's disease: a PET follow-up study. *European Journal of Nuclear Medicine and Molecular Imaging*, 30, 1104–1113.

Evans, A. D. *et al.* (1994). 3D statistical neuroanatomical models from 305 MRI volumes. *IEEE Nuclear Science Symposium Medical Imaging Conference*, 3, 1813–1817.

Fellgiebel, A., Scheurich, A., Bartenstein, P. and Muller, M. J. (2007). FDG-PET and CSF phospho-tau for prediction of cognitive decline in mild cognitive impairment. *Psychiatry Research*, 155, 167–171.

Folstein, M. F., Folstein, S. E. and McHugh, P. R. (1975). "Mini-mental state": a practical method for grading the cognitive state of patients for the clinician. *Journal of Psychiatric Research*, 12, 189–198.

Hoffman, J. M. *et al.* (2000). FDG PET imaging in patients with pathologically verified dementia. *Journal of Nuclear Medicine*, 41, 1920–1928.

Ishiwata, A., Sakayori, O., Minoshima, S., Mizumura, S., Kitamura, S. and Katayama, Y. (2006). Preclinical evidence of Alzheimer changes in progressive mild cognitive impairment: a qualitative and quantitative SPECT study. *Acta Neurologica Scandinavica*, 114, 91–96.

Larrieu, S. *et al.* (2002). Incidence and outcome of mild cognitive impairment in a population-based prospective cohort. *Neurology*, 59, 1594–1599.

McKhann, G., Drachman, D., Folstein, M., Katzman, R., Price, D. and Stadlan, E. M. (1984). Clinical diagnosis of AD: report of the NINCDS-ADRDA work group under the auspices of department of health and human services task force on AD. *Neurology*, 34, 939–944.

Meguro, K. (2004). *A Clinical Approach to Dementia: An Instruction of CDR Worksheet*. Tokyo: Igaku-Shoin.

Meguro, K. *et al.* (2002). Prevalence of dementia and dementing diseases in Japan: the Tajiri Project. *Archives of Neurology*, 59, 1109–1114.

Meguro, K. *et al.* (2004). Prevalence and cognitive performances of Clinical Dementia Rating 0.5 and mild cognitive impairment in Japan: the Tajiri Project. *Alzheimer Disease and Associate Disorders*, 18, 3–10.

Meguro, K. *et al.* (2007) Incidence of dementia and associated risk factors in Japan: The Osaki-Tajiri Project. *Journal of Neurological Sciences*, 260, 175–182.

Morris, J. C. (1993). The Clinical Dementia Rating (CDR): current version and scoring rules. *Neurology*, 43, 2412–2414.

Morris, J. C. *et al.* (2001). Mild cognitive impairment represents early-stage Alzheimer's disease. *Archives of Neurology*, 58, 397–405.

Mosconi, L. *et al.* (2004). MCI conversion to dementia and the APOE genotype: a prediction study with FDG-PET. *Neurology*, 63, 2332–2340.

Perneczky, R., Hartmann, J., Grimmer, T., Drzezga, A. and Kurz, A. (2007). Cerebral metabolic correlates of the Clinical Dementia Rating scale in mild cognitive impairment. *Journal of Geriatric Psychiatry and Neurology*, 20, 84–88.

Petersen, R. C., Smith, G. E., Waring, S. C., Ivnik, R. J., Kokmen, E. and Tangelos, E. G. (1997). Aging, memory, and mild cognitive impairment. *International Psychogeriatrics*, 9, 65–69.

Phelps, M. E., Huang, S. C., Hoffman, E. J., Selin, C., Sokoloff, L. and Kuhl, D. E. (1979). Tomographic measurement of local glucose metabolic rate in humans with (FO-18)2-fluoro-2-deoxy-D-glucose: validation of method. *Annals of Neurology*, 6, 371–388.

Reisberg, B., Ferris, S. H. and de Leon, M. J. (1982). The global deterioration scale for assessment of primary degenerative dementia. *American Journal of Psychiatry*, 139, 1136–1139.

Reivich, M. *et al.* (1979). The ^{18}F-fluoro-deoxyglucose method for the measurement of local cerebral glucose utilization in man. *Circulation Research*, 44, 127–137.

Silverman, D. H. *et al.* (2001). Positron emission tomography in evaluation of dementia: regional brain metabolism and long-term outcome. *JAMA*, 286, 2120–2127.

Talairach, J. and Trournoux, P. (1988). *Co-planar Stereotaxic Atlas of the Human Brain: 3-dimensional Proportional System: An Approach to Cerebral Imaging*. New York: Thieme Medical.

Teng, E. L. *et al.* (1994). The Cognitive Ability Screening Instrument (CASI): a practical test for cross-cultural epidemiological studies of dementia. *International Psychogeriatrics*, 6, 45–58.

Visser, P. J., Verhey, F. R., Hofman, P. A., Scheltens, P. and Jolles, J. (2002). Medial temporal lobe atrophy predicts Alzheimer's disease in patients with minor cognitive impairment. *Journal of Neurology, Neurosurgery, and Psychiatry*, 72, 491–497.

Yamaguchi, S. *et al.* (1997). Decreased cortical glucose metabolism correlated with hippocampal atrophy in Alzheimer's disease as shown by MRI and PET. *Journal of Neurology, Neurosurgery, and Psychiatry*, 62, 596–600.

Ann Nucl Med (2008) 22:841–847
DOI 10.1007/s12149-008-0185-5

ORIGINAL ARTICLE

Adenosine A_1 receptors using 8-dicyclopropylmethyl-1-[^{11}C]methyl-3-propylxanthine PET in Alzheimer's disease

**Nobuyoshi Fukumitsu · Kenji Ishii · Yuichi Kimura
Keiichi Oda · Masaya Hashimoto · Masahiko Suzuki
Kiichi Ishiwata**

Received: 5 September 2007 / Accepted: 19 June 2008

Abstract
Objective Adenosine is an endogenous modulator of synaptic functions in the central nervous system. The effects of adenosine are mediated by at least four adenosine receptor subtypes. Decreased density of adenosine A_1 receptors, which is a major subtype adenosine receptor in the hippocampus, has been reported in vitro in Alzheimer's disease. We evaluated adenosine A_1 receptor in the brain of elderly normal subjects and patients with Alzheimer's disease (n = 8 and 6, respectively), using positron emission tomography (PET) and 8-dicyclopropylmethyl-1-[^{11}C]methyl-3-propylxanthine ([^{11}C]MPDX).
Methods A 60-min PET scan with [^{11}C]MPDX was performed. The patients with Alzheimer's disease also underwent PET with [^{18}F]fluorodeoxyglucose (FDG). The binding potential of [^{11}C]MPDX was quantitatively calculated in the regions of interest (ROIs) placed on the frontal, medial frontal, temporal, medial temporal, parietal, and occipital cortices, striatum, thalamus, cerebellum, and pons. Statistical parametric mapping (SPM2) was used for analysis of [^{11}C]MPDX and FDG-PET.
Results In the ROI-based analysis, the binding potential of [^{11}C]MPDX in patients with Alzheimer's disease was significantly lower in the temporal and medial temporal cortices and thalamus than that in elderly normal subjects (P = 0.038, 0.028, and 0.039, respectively). SPM analysis also showed significant decreased binding potential in the temporal and medial temporal cortices and thalamus in patients with Alzheimer's disease. FDG uptake was significantly decreased in the temporoparietal cortex and posterior cingulate gyrus.
Conclusions Decreased binding of [^{11}C]MPDX in patients with Alzheimer's disease was detected in temporal and medial temporal cortices and thalamus. This pattern possibly differed from the hypometabolism pattern of FDG. [^{11}C]MPDX PET is valuable for the detection of degeneration in the temporal and medial temporal cortices and corticothalamic transmission, and may provide a different diagnostic tool from FDG-PET in brain disorders such as Alzheimer's disease.

Keywords [^{11}C]MPDX · Adenosine A_1 receptor · Medial temporal cortex · Positron emission tomography · Alzheimer's disease

N. Fukumitsu (✉)
2-1-1-204 Midoridai, Funabashi, Chiba 274-0818, Japan
e-mail: fukumitsun@yahoo.co.jp

N. Fukumitsu
Proton Medical Research Center, University of Tsukuba, Ibaraki, Japan

N. Fukumitsu · K. Ishii · Y. Kimura · K. Oda · K. Ishiwata
Positron Medical Center, Tokyo Metropolitan Institute of Gerontology, Tokyo, Japan

M. Hashimoto · M. Suzuki
Department of Neurology, Jikei University School of Medicine, Tokyo, Japan

Introduction

Adenosine is present in large amounts in the mammalian brain and plays a role as an endogenous modulator of synaptic functions in the central nervous system. Prior work has established a role for adenosine in a diverse array of neural phenomena, which include regulation of

sleep and the level of arousal, neuroprotection, regulation of seizure susceptibility, locomotor effects, analgesia, mediation of the effects of ethanol, and chronic drug use [1]. Therefore, interaction with the adenosine metabolism is a promising target for therapeutic intervention in ischemic, neurological, and psychiatric disorders [2–4].

The effects of adenosine are mediated by at least four adenosine receptor subtypes, namely, A_1, A_{2A}, A_{2B}, and A_3. The two major subtypes of receptors, namely, A_1 and A_2 receptors, have been well investigated in molecular biology, pharmacology, and physiology [4–6]. Adenosine presynaptically inhibits the release of many neurotransmitters, especially excitatory ones such as the potentially excitotoxic amino acid glutamate [7, 8]. This effect of adenosine is mediated by presynaptic A_1 receptors linked via G-proteins to both calcium and potassium ion channels [9–12].

Alzheimer's disease is the most common form of age-related dementia and one of the most serious health problems. Dementia affects approximately 1–5% of the population more than 65 years of age [13] and 20–40% of the population more than 80 years of age [14, 15]. The economic and social burdens of Alzheimer's disease on families have been documented in many studies [16–18]. In studies on the postmortem brain with Alzheimer's disease, decreased density of adenosine A_1 receptor in the hippocampus has been reported [19–22]. Ulas et al. [20] reported that the reduction in the adenosine A_1-specific ligand-receptor binding was owing to a decrease in the density of binding sites (B_{max}), but was not owing to changes in the affinity (K_d) [20]. With regard to the clinical diagnosis of Alzheimer's disease, positron emission tomography (PET) using [^{18}F]fluorodeoxyglucose (FDG) is the most popular method, and reduction of glucose metabolism is prominent in the temporo-parietal cortex and posterior cingulate gyrus. However, hypometabolism in the medial temporal cortex has not necessarily been detected as a symptom of Alzheimer's disease, although morphological changes are prominent in the medial temporal cortex [23–25].

Recently, we successfully performed imaging of adenosine A_1 receptors in the human brain of normal young volunteers using PET with 8-dicyclopropylmethyl-1-[^{11}C]methyl-3-propylxanthine ([^{11}C]MPDX) [26–29]. In the present study, we investigated the change of the adenosine A_1 receptors in patients with Alzheimer's disease with [^{11}C]MPDX PET. We also examined the same patients with FDG-PET for direct comparison of the two diagnostic tools. This report is a preliminary study of the utility of [^{11}C]MPDX PET in the diagnosis of patients with Alzheimer's disease.

Materials and methods

The study protocol was approved by the Institutional Ethical Committee. Eight normal elderly volunteers [men 66.9 ± 6.5 (61–75) years] were enrolled together with six Alzheimer's disease patients [men, $n = 5$; women, $n = 1$; 73.5 ± 9.8 (58–83) years]. A written informed consent was obtained from all the participants in this study. It was confirmed that no participants received xanthine-type drugs such as theophylline for asthma.

All the normal subjects were healthy according to the history, physical, neurological and psychiatric examinations, and a magnetic resonance imaging (MRI) study of the brain prior to the PET study. In the psychiatric examination, we used the Hospital Anxiety and Depression Scale [30].

All the patients with Alzheimer's disease showed mild-to-moderate dementia and were diagnosed according to the National Institute of Neurological and Communicative Diseases and Stroke/Alzheimer's Disease and Related Disorders Association (NINCDS–ADRDA) criteria. The disease duration following the first onset of memory disturbance was 0–4 years. We performed clinical assessments, including neuropsychological testing and exclusion of other diseases, with computed tomography or MRI as required by the NINCDS–ADRDA criteria. The exclusion criteria were prior episodes of subarachnoid or intracerebral hemorrhage, intracranial tumors, hydrocephalus, all psychoses (including major depression), alcoholism, epilepsy, ischemic strokes, vascular dementia, sleep disorders, and other forms of dementia, anemia, and nonstabilized diabetes mellitus. The patients who were suspected to have other diseases with neurodegeneration from the FDG-PET findings or who were on medications that affect the brain circulation or metabolism were excluded, and especially acethylcholinesterase blockers were not given prior to the PET study. The Mini-Mental State Examination score was 20–24. Neither normal subjects nor patients with Alzheimer's disease complained about their sleep behavior.

PET measurement

Radiosynthesis of [^{11}C]MPDX was performed as described earlier [31, 32]. PET measurement was performed with an SET-2400W system (Shimadzu, Kyoto, Japan), which acquires 63 slices having 128 × 128 pixels each at a transverse resolution of 4.5 mm full width at half maximum (FWHM) and at an axial resolution of 5.8 mm FWHM. Scanning took place as the subjects lay supine. A venous catheter was inserted into the forearm vein of the subjects for tracer injection, and an arterial

catheter was inserted into the distal radial artery under local anesthesia for arterial blood sampling. After positioning the subject's head in the canthomeatal orientation and fixing the subject's head using a band to prevent movement during the examination, a transmission scan was performed with a rotating [^{68}Ga]/[^{68}Ge] line source to correct for the photon attenuation using the attenuation map. All the subjects were given [^{11}C]MPDX [611 ± 123 (300–757) MBq/14.4 ± 12.5 (2.8–47.5 nmol)] for a period of 10 s, and the PET scan and arterial blood sampling were performed for 60 min as described earlier [27]. We did not impose any meal restriction for [^{11}C]MPDX PET.

In all patients with Alzheimer's disease, FDG-PET was also done on the same day or within 3 months. The subjects each received an intravenous injection of FDG [128 ± 13 (107–142) MBq]. Starting 45 min post-injection, an emission scan was performed for 6 min following a transmission scan using ^{68}Ge for attenuation correction. In the case of one of the six patients who underwent both [^{11}C]MPDX PET and FDG-PET on the same day, the former was carried out in the morning, with FDG administered 3 h later.

Kinetic analysis

The PET images were registered and resliced to the MRI with Ardekani's-image registration algorithm [33] using UNIX workstations (Silicon Graphics, Mountain View, CA, USA) with the Dr. View image analysis software system (AJS, Tokyo, Japan). Regions of interest (ROIs) were placed on the frontal, medial frontal, temporal, medial temporal, parietal, and occipital cortices, striatum, thalamus, cerebellum, and pons based on MRI (Fig. 1). The ROI on the frontal cortex had 1582 ± 275 voxels and that on the pons had 85 ± 3 voxels (1 voxel = 2 mm × 2 mm × 6.25 mm). The voxel numbers on other regions were in-between these values. Using the time–activity curves for each ROI of the brain and the metabolite-corrected time–activity curve of plasma, the distribution volume (DV) of [^{11}C]MPDX in each ROI was calculated by graphical analysis using Logan plots according to the method as described earlier [27, 28]. The binding potential in each ROI was then obtained as follows [28]:

$$\text{Binding potential} = DV_{(\text{region})}/DV_{(\text{cerebellum})} - 1.$$

The binding potential in each ROI was expressed as mean values ± standard deviations. The difference of the binding potential in each ROI was respectively tested between normal elderly subjects group and patients with Alzheimer's disease group using Mann–Whitney *U* test.

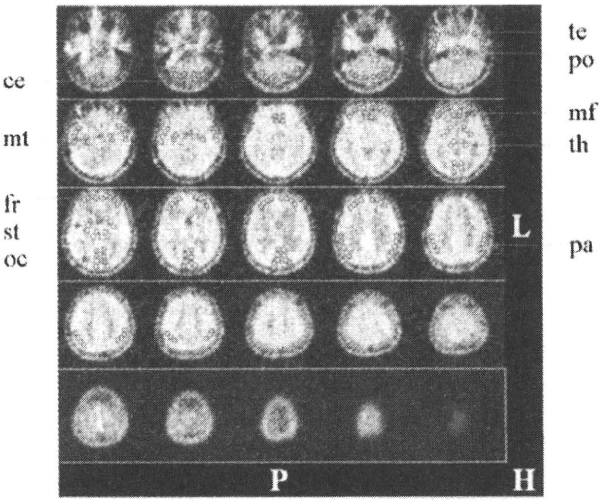

Fig. 1 Region of interest mapping of 8-dicyclopropylmethyl-1-[^{11}C]methyl-3-propylxanthine positron emission tomography ([^{11}C]MPDX PET). *fr* frontal cortex, *mf* medial frontal cortex, *te* temporal cortex, *mt* medial temporal cortex, *pa* parietal cortex, *oc* occipital cortex, *st* striatum, *th* thalamus, *ce* cerebellum, *po* pons

Statistical significance was assumed at $P < 0.05$. In FDG-PET, regional glucose metabolism was expressed using standardized uptake value (SUV).

Statistical parametric mapping analysis

The PET images were analyzed using SPM2 software (Wellcome Department of Cognitive Neurology, Institute of Neurology, London, UK), implemented using Matlab 7.0 (MathWorks, Sherborn, MA, USA). For this purpose, binding potential image of [^{11}C]MPDX and SUV image of FDG were used. Prior to statistical analysis, all the images were spatially normalized into the MNI standard space (Montreal Neurological Institute, McGill University, Montreal, QC, Canada) using house-made templates for [^{11}C]MPDX and FDG-PET images, to remove inter-subject anatomical variability. In normalization of [^{11}C]MPDX PET, total DV image that well reflected brain anatomical structure including cerebellum was used. Spatially normalized images were smoothed by convolution, using an isotropic Gaussian kernel with 16 mm FWHM. The aim of smoothing was to increase the signal-to-noise ratio and to account for the subtle variations in anatomical structures. The count of each voxel in FDG-PET was normalized to the global mean (value = 50) with proportional scaling in SPM2. No global normalization was applied to the [^{11}C]MPDX PET because binding potential was quantitatively calculated. After spatial and count normalization, statistical comparisons between groups were performed on a voxel-by-voxel basis using *t* statistics, generating SPM (*t*)

maps. In FDG-PET, the data of the normal elderly template in our institute (n = 41, 51–78 years) were used as a reference for the patients with Alzheimer's disease. The data of the normal volunteers whose age and eligibility were matched with this protocol were used in normal elderly template. Thresholds of $P < 0.005$ and $P < 0.01$ corrected for the cluster level were applied to [^{11}C]MPDX and FDG-PET images, respectively. The clusters with an extent of greater than 300 voxels were considered. For visualization of the t score statistics [SPM (t) map], the significant voxels were projected onto the 3D rendered brain of a standard high-resolution MRI template provided by SPM2, thus allowing anatomical identification.

Results

In the ROI-based analysis, the binding potential of [^{11}C]MPDX in normal elderly subjects was high in the striatum and thalamus and low in the cerebellum and pons. The binding potential of [^{11}C]MPDX in patients with Alzheimer's disease was high in the striatum and thalamus and low in the medial temporal cortex and cerebellum. The binding potential of [^{11}C]MPDX in patients with Alzheimer's disease was significantly lower in the temporal, medial temporal cortices, and thalamus than that in normal elderly subjects (P = 0.038, 0.028, and 0.039, respectively; Fig. 2). Especially, the binding potential of [^{11}C]MPDX in the medial temporal cortex in patients with Alzheimer's disease was nearly equal to that in the cerebellum.

The SPM analysis of [^{11}C]MPDX PET between patients with Alzheimer's disease and normal elderly subjects is shown in Fig. 3a. The binding potential was widely and severely decreased in the temporal, medial temporal cortices, and thalamus, and partially decreased in the parietal cortex in patients with Alzheimer's disease with significance ($P < 0.005$, corrected $k > 300$). Decreased binding potential was slightly prominent in the left hemisphere.

The SPM analysis of FDG-PET in the same patients with Alzheimer's disease is shown in Fig. 3b. The FDG uptake was widely and severely decreased in the temporoparietal cortex and posterior cingulate gyrus with significance ($P < 0.01$, corrected $k > 300$). Decreased FDG uptake was slightly prominent in the left hemisphere.

Discussion

In Alzheimer's disease subjects, ROI-based analysis and SPM analysis clearly demonstrated the decreased binding potential of [^{11}C]MPDX in the temporal and medial temporal cortices and thalamus when compared with normal elderly subjects as shown in Figs. 2 and 3a. The finding of decreased binding potential in the medial temporal cortex is consistent with past postmortem autoradiographic and pathological studies of patients with Alzheimer's disease [19–22]. Ulas et al. [20] reported that decreased A_1 agonist binding was observed in the CA1 stratum oriens and outer layers of the parahippocampal gyrus, whereas decreased antagonist binding was found in the subiculum and CA3 region. Adenosine A_1 recep-

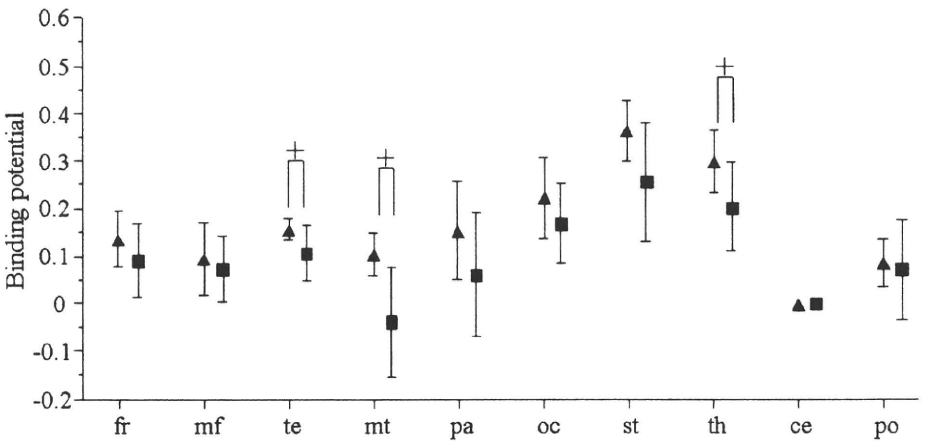

Fig. 2 Binding potential of [^{11}C]MPDX in the human brain. Patients with Alzheimer's disease showed a significantly lower value in the temporal and medial temporal cortices and thalamus than normal elderly volunteers. The value in the cerebellum was zero because the value was calculated based on the assumption that adenosine A_1 receptors are very sparse in the cerebellum. Abbreviations used are the same as in Fig. 1. *Triangle* normal elderly subjects (n = 8), *square* patients with Alzheimer's disease (n = 6), *plus* $P < 0.05$ compared between normal elderly subjects and patients with Alzheimer's disease

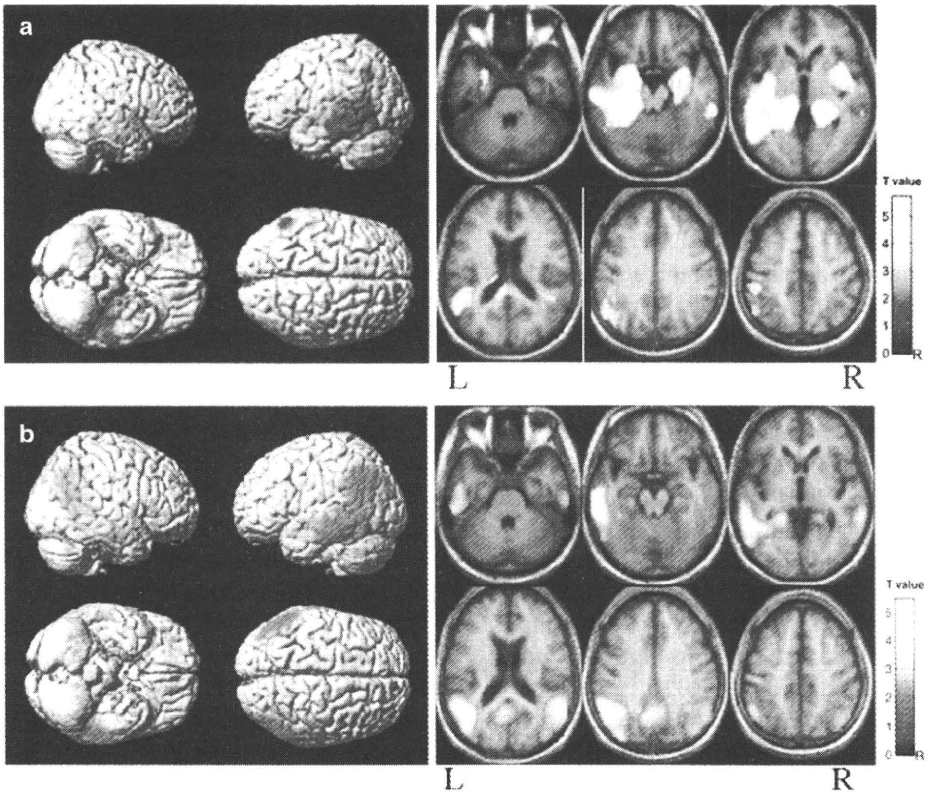

Fig. 3 Statistical analyses of the binding potential of [^{11}C]MPDX (**a**) and standardized uptake value (SUV) of [^{18}F]fluorodeoxyglucose (FDG, **b**) in patients with Alzheimer's disease. *Left* Statistical parametric mapping (SPM) *Z* maps are superimposed onto the right lateral, left lateral, inferior, and superior views (from *left upper* to *right lower*) of a volume-rendered spatially normalized magnetic resonance imaging (MRI) study. *Right* SPM *Z* maps are superimposed onto the axial views of a spatially normalized T1-MRI study. Each image represents from the *bottom* (*left upper*) to the *top* (*right lower*). *Red* and *yellow* represent the areas with significant reduction in binding potential or SUV. **a** Decreased binding potential of [^{11}C]MPDX was noted in the temporal, medial temporal cortices, and thalamus widely and parietal cortex partially. Decreased binding is slightly prominent in the left hemisphere. **b** Decreased SUV of FDG was noted in the temporo-parietal cortices. Decreased SUV is slightly prominent in the left hemisphere

tors are located on the terminal of the perforant pathway which provides a major input to the molecular layer of the dentate gyrus [34]. It has been reported that the perforant pathway contributes 80%–85% of the synapses on the outer portion of the dendrites that arise from the dentate gyrus granule cells [34, 35]. The cells of origin of the perforant pathway in the entorhinal cortex are destroyed in the brain of patients with Alzheimer's disease [34]. Decreased binding potential of [^{11}C]MPDX in the medial temporal cortex is considered to be affected by insufficiency or damage to the perforant pathway in patients with Alzheimer's disease. Decreased binding potential of [^{11}C]MPDX in the temporal cortex in patients with Alzheimer's disease can be directly or indirectly correlated with destruction of the cells of origin of the perforant pathway. Thalamic nuclei have strong reciprocal connections with the cerebral cortex, forming thalamo-cortico-thalamic circuits. An abnormal finding in the thalamus of Alzheimer's disease has been described in a few MRI reports [36, 37]. It is considered that decreased binding potential of [^{11}C]MPDX in the thalamus is derived from corticothalamic transmission from the temporal and medial temporal cortices. The reason for the laterality in [^{11}C]MPDX and FDG-PET can be derived from investigations of small numbers ($n = 6$) of patients. Laterality in FDG-PET was also reported in a study with a small number of patients with Alzheimer's disease [38]. It is necessary to investigate these issues in greater number of patients.

We calculated the binding potential as a reference for the cerebellar cortex because the cerebellar cortex showed very low adenosine A_1 receptor densities [39] and this method provided well-balanced data in our earlier study [28]. The calculated binding potential of [^{11}C]MPDX in the medial temporal cortex was slightly lower than 0, which means that adenosine A_1 receptor density in the

medial temporal cortex in patients with Alzheimer's disease is nearly equal to or lower than that in the cerebellar cortex which contains very low adenosine A_1 receptor densities [39]. A severely decreased binding potential of [^{11}C]MPDX in the medial temporal cortex means that the perforant pathway in the medial temporal cortex is markedly insufficient or damaged in patients with Alzheimer's disease.

We consider that the decreased binding potential of [^{11}C]MPDX in the temporal and medial temporal cortices directly or indirectly reflects insufficiency or damage to the perforant pathway. On the other hand, the SPM analysis of FDG-PET findings in the present study revealed that FDG uptake was decreased in the temporal cortex and not in the medial temporal cortex, where the binding potential of [^{11}C]MPDX decreased markedly. The findings suggested that insufficiency or damage to the perforant pathway in the medial temporal cortex could not necessarily be reflected by the FDG-PET results.

Hypometabolism in the temporo-parietal cortex and posterior cingulate gyrus (Fig. 3b) is a typical pattern revealed by FDG-PET in Alzheimer's disease subjects [23–25, 40, 41]. In the temporo-parietal cortex, the area with severe hypometabolism was obviously larger than that with decreased binding potential of [^{11}C]MPDX in patients with Alzheimer's disease. In the posterior cingulate gyrus, [^{11}C]MPDX PET was not coupled with hypometabolism. Therefore, FDG-PET is more sensitive in detecting the degeneration of the temporo-parietal cortex and posterior cingulate gyrus, which is a typical manifestation in Alzheimer's disease, than [^{11}C]MPDX PET. However, it is well known that FDG-PET in Alzheimer's disease does not necessary reflect the pathological changes [42–44]. [^{11}C]MPDX PET provides a different diagnostic tool than FDG-PET, and could be valuable in detecting the degeneration in the medial temporal cortex. In addition, [^{11}C]MPDX PET has the possibility to detect corticothalamic transmission from the temporal and medial temporal cortices.

Conclusions

In patients with Alzheimer's disease, the binding potential of [^{11}C]MPDX decreased significantly in the temporal and medial temporal cortices and thalamus, and a small or no decrease was observed in the parietal cortex and posterior cingulate gyrus. The pattern of the binding potential of [^{11}C]MPDX had the possibility to be different from that of the FDG-PET in patients with Alzheimer's disease.

Acknowledgments This work was supported by Grants-in-Aid for Scientific Research (B) Nos. 16390348 and 20390334 from the Japan Society for the Promotion of Science. The authors thank Dr. Kazunori Kawamura for the preparation of [^{11}C]MPDX and Ms. Miyoko Ando for her care of the subjects during the PET measurement.

References

1. Dunwiddie TV, Masino SA. The role and regulation of adenosine in the central nervous system. Ann Rev Neurosci 2001; 24:31–55.
2. Yacoubi ME, Costentin J, Vaugeois JM. Adenosine A_{2A} receptors and depression. Neurology 2003;61:S82–7.
3. von Lubitz DK. Adenosine in the treatment of stroke: yes, maybe, or absolutely not? Expert Opin Investig Drugs 2001; 10:619–32.
4. Haas HL, Selbach O. Functions of neuronal adenosine receptors. Naunyn Schmiedebergs Arch Pharmacol 2000;362: 375–81.
5. Collis MG, Hourani SMO. Adenosine receptor subtypes. Trends Pharmacol Sci 1993;14:360–6.
6. Fredholm BB, Abbracchio MP, Burnstock G, Daly JW, Harden TK, Jacobson KA, et al. Nomenclature and classification of purinoceptors. Pharmacol Rev 1994;46:143–56.
7. Corradetti R, Lo Conte G, Moroni F, Passani MB, Pepeu G. Adenosine decreases aspartate and glutamate release from rat hippocampal slices. Eur J Pharmacol 1984;104:19–26.
8. Dolphin AC, Archer ER. An adenosine agonist inhibits and a cyclic AMP analogue enhances the release of glutamate but not GABA from slices of rat dentate gyrus. Neurosci Lett 1983;43:49–54.
9. Dunwiddie TV. The physiological role of adenosine in the central nervous system. Int Rev Neurobiol 1985;27:63–139.
10. Fredholm BB, Dunwiddie TV. How does adenosine inhibit transmitter release? Trends Pharmacol Sci 1988;9:130–4.
11. Fredholm BB, Hedqvist P. Modulation of neurotransmission by purine nucleotides and nucleosides. Biochem Pharmacol 1980;29:1635–43.
12. Phillis JW, Wu PH. The role of adenosine and its nucleotides in central synaptic transmission. Prog Neurobiol 1981;16: 187–239.
13. Schoenberg BS. Epidemiology of Alzheimer's disease and other dementing disorders. J Chronic Dis 1986;39:1095–104.
14. Fratiglioni L, Grut M, Forsell Y, Viitanen M, Grafstrom M, Holmen K, et al. Prevalence of Alzheimer's disease and other dementias in an elderly urban population: relationship with age, sex, and education. Neurology 1991;41:1886–92.
15. Brookmeyer R, Gray S, Kawas C. Projections of Alzheimer's disease in the United States and the public health impact of delaying disease onset. Am J Public Health 1998;88:1337–42.
16. Weinberger M, Gold DT, Divine GW, Cowper PA, Hodgson LG, Schreiner PJ, et al. Expenditures in caring for patients with dementia who live at home. Am J Public Health 1993; 83:338–41.
17. Osttbye T, Crosse E. Net economic costs of dementia in Canada. CMAJ 1994;151:1457–63.
18. Ernst R, Hay JW, Fenn C, Tinklenberg J, Yesavage JA. Cognitive function and the costs of Alzheimer's disease. Arch Neurol 1997;54:687–93.
19. Jansen K, Faull RLM, Dragunow M, Synek BJL. Alzheimer's disease: changes in hippocampal *N*-methyl-D-aspartate, quisqualate, neurotensin, adenosine, benzodiazepine, sero-

tonin and opioid receptors: an autoradiographic study. Neuroscience 1990;39:613–27.
20. Ulas J, Brunner LC, Nguyen L, Cotman CW. Reduced density of adenosine A1 receptors and preserved coupling of adenosine A1 receptors to G proteins in Alzheimer hippocampus: a quantitative autoradiographic study. Neuroscience 1993;52: 843–54.
21. Jaarsma D, Sebens B, Korf J. Reduction of adenosine A1-receptors in the perforant pathway terminal zone in Alzheimer hippocampus. Neurosci Lett 1991;121:111–4.
22. Kalaria RN, Sromek S, Wilcox BJ, Unnerstall JR. Hippocampal adenosine A1 receptors are decreased in Alzheimer's disease. Neurosci Lett 1990;118:257–60.
23. Ishii K, Sasaki H, Kono AK, Miyamoto N, Fukuda T, Mori E. Comparison of gray matter and metabolic reduction in mild Alzheimer's disease using FDG-PET and voxel-based morphometric MR studies. Eur J Nucl Med 2005;32:959–63.
24. Mosconi L. Brain glucose metabolism in the early and specific diagnosis of Alzheimer's disease. FDG-PET studies in MCI and AD. Eur J Nucl Med 2005;32:486–510.
25. Meguro K, LeMestric C, Landeau B, Desgranges B, Eustache F, Baron JC. Relations between hypometabolism in the posterior association neocortex and hippocampal atrophy in Alzheimer's disease: a PET/MRI correlative study. J Neurol Neurosurg Psychiatry 2001;71:315–21.
26. Fukumitsu N, Ishii K, Kimura Y, Oda K, Sasaki T, Mori Y, et al. Imaging of adenosine A_1 receptors in the human brain by positron emission tomography with [^{11}C]MPDX. Ann Nucl Med 2003;17:511–5.
27. Fukumitsu N, Ishii K, Kimura Y, Oda K, Sasaki T, Mori Y, et al. Adenosine A_1 receptor mapping of the human brain by PET with 8-dicyclopropylmethyl-1-11C-methyl-3-propylxanthine. J Nucl Med 2005;46:32–7.
28. Kimura Y, Ishii K, Fukumitsu N, Oda K, Sasaki T, Kawamura K, et al. Quantitative analysis of adenosine A_1 receptors in human brain using positron emission tomography and [1-methyl-^{11}C]8-dicyclopropylmethyl-1-methyl-3-propylxanthine. Nucl Med Biol 2004;31:975–81.
29. Naganawa M, Kimura Y, Nariai T, Ishii K, Oda K, Manabe Y, et al. Omission of serial arterial blood sampling in neuroreceptor imaging with independent component analysis. Neuroimage 2005;26:885–90.
30. Zigmond AS, Snaith RP. The Hospital Anxiety and Depression Scale. Acta Psychiatr Scand 1983;67:361–7.
31. Noguchi J, Ishiwata K, Furuta R, Simada J, Kiyosawa M, Ishii S, et al. Evaluation of carbon-11 labeled KF15372 and its ethyl and methyl derivatives as a potential CNS adenosine A_1 receptor ligand. Nucl Med Biol 1997;24:53–9.
32. Ishiwata K, Nariai T, Kimura Y, Oda K, Kawamura K, Ishii K, et al. Preclinical studies on [^{11}C]MPDX for mapping adenosine A_1 receptors by positron emission tomography. Ann Nucl Med 2002;16:377–82.
33. Ardekani BA, Braun M, Hutton BF, Kanno I, Iida H. A fully automatic multimodality image registration algorithm. J Comput Assist Tomog 1995;19:615–23.
34. Dragunow M, Murphy K, Leslie RA, Robertson HA. Localization of adenosine A1-receptors to the terminals of the perforant path. Brain Res 1988;462:252–7.
35. Hyman BT, Van Hoesen GW, Kromer LJ, Damasio AR. Perforant pathway changes and the memory impairment of Alzheimer's disease. Ann Neurol 1986;20:472–81.
36. Stephen RE, Janke AL, Chark JB. Gray and white matter changes in Alzheimer's disease: a diffusion tensor imaging study. J Magn Reson Imaging 2008;27:20–6.
37. Medina D, DeToledo-Morrell L, Urresta F, Gabrieli JD, Moseley M, Fleischman D, et al. White matter changes in mild cognitive impairment and AD: a diffusion tensor imaging study. Neurobiol Aging 2006;27:663–72.
38. Zahn R, Juengling F, Bubrowski P, Jost E, Dykierek P, Talazko J, et al. Hemisphere asymmetries of hypometabolism associated with semantic memory impairment in Alzheimer's disease: a study using positron emission tomography with fluorodeoxygulcose-F18. Psychiatry Res Neuroimaging 2004; 132:159–72.
39. Fastbom J, Pazos A, Probst A, Palacios JM. Adenosine A1 receptors in the human brain: a quantitative autoradiographic study. Neuroscience 1987;22:827–39.
40. Sakamoto S, Ishii K, Sasaki M, Hosaka M, Mori T, Matsui M, et al. Differences in cerebral metabolic impairment between early and late onset types of Alzheimer's disease. J Neurol Sci 2002;15:27–32.
41. Kim EJ, Cho SS, Jeong Y, Park KC, Kang E, Kim SE, et al. Glucose metabolism in early onset versus late onset Alzheimer's disease: an SPM analysis of 120 patients. Brain 2005;128:1790–801.
42. Ibanez V, Pietrini P, Alexander GE, Furey ML, Teichberg D, Rajapakse JC, et al. Regional glucose metabolic abnormalities are not the result of atrophy in Alzheimer's disease. Neurology 1998;50:1585–93.
43. Mosconi L, Sorbi S, de Leon MJ, Li Y, Nacmias B, Myoung PS, et al. Hypometabolism exceeds atrophy in presymptomatic early-onset familial Alzheimer's disease. J Nucl Med 2006;47:1778–86.
44. Chetelat G, Desgranges B, Landeau B, Mezenge F, Poline JB, de la Sayette V, et al. Direct voxel-based comparison between grey matter hypometabolism and atrophy in Alzheimer's disease. Brain 2008;131:60–71.

Ann Nucl Med (2008) 22:151–156
DOI 10.1007/s12149-007-0094-z

ORIGINAL ARTICLE

Low density of sigma$_1$ receptors in early Alzheimer's disease

**Masahiro Mishina · Masashi Ohyama · Kenji Ishii
Shin Kitamura · Yuichi Kimura · Kei-ichi Oda
Kazunori Kawamura · Toru Sasaki · Shiro Kobayashi
Yasuo Katayama · Kiichi Ishiwata**

Received: 24 July 2007 / Accepted: 5 September 2007

Abstract
Objective The sigma$_1$ receptor is considered to be involved in cognitive function. A postmortem study reported that the sigma$_1$ receptors were reduced in the hippocampus in Alzheimer's disease (AD). However, in vivo imaging of sigma$_1$ receptors in the brain of AD patients has not been reported. The aim of this study is to investigate the mapping of sigma$_1$ receptors in AD using [^{11}C]SA4503 positron emission tomography (PET).

Methods We studied five AD patients and seven elderly volunteers. A dynamic series of decay-corrected PET data acquisition was performed for 90 min starting at the time of the injection of 500 MBq of [^{11}C]SA4503. A two-tissue three-compartment model was used to estimate K_1, k_2, k_3, k_4, and the delay between metabolite-corrected plasma and tissue time activity using a Gauss–Newton algorithm. The ratio of k_3 to k_4 was computed as the binding potential (BP), which is linearly related to the density of sigma$_1$ receptors. Unpaired t tests were used to compare K_1 and BP in patients with AD and normal subjects.
Results As compared with normals, BP in the AD was significantly lower in the frontal, temporal, and occipital lobe, cerebellum and thalamus, whereas K_1 was significantly lower in the parietal lobe.
Conclusions [^{11}C]SA4503 PET can demonstrate that the density of cerebral and cerebellar sigma$_1$ receptors is reduced in early AD.

Keywords Alzheimer's disease · Positron emission tomography · Sigma$_1$ receptor · Cortex · Cerebellum

M. Mishina · M. Ohyama · K. Ishii · Y. Kimura · K. Oda · K. Kawamura · T. Sasaki · K. Ishiwata
Positron Medical Center, Tokyo Metropolitan Institute of Gerontology, Tokyo, Japan

M. Mishina · M. Ohyama · S. Kitamura · Y. Katayama
Department of Neurology, Nephrology and Rheumatology, Nippon Medical School, Tokyo, Japan

M. Mishina (✉) · S. Kobayashi
Neurological Institute, Nippon Medical School Chiba-Hokusoh Hospital, 1715 Kamagari, Imba-mura, Imba-gun, Chiba 270-1694, Japan
e-mail: mishina@nms.ac.jp

S. Kitamura
Department of Internal Medicine, Nippon Medical School Musashi Kosugi Hospital, Kanagawa, Japan

Y. Kimura
Biophysics Group, Molecular Imaging Center, National Institute of Radiological Sciences, Chiba, Japan

K. Kawamura
Center for Integrated Brain Science, Brain Research Institute, University of Niigata, Niigata, Japan

T. Sasaki
Research Team for Molecular Biomarkers, Tokyo Metropolitan Institute of Gerontology, Tokyo, Japan

Introduction

Sigma$_1$ receptor has received considerable attention in the regulation of cognitive function [1]. The sigma receptor has been established as a distinct receptor, although it was initially proposed as a subtype of opioid receptors [2]. It is classified into at least two subtypes, namely, sigma$_1$ and sigma$_2$ [3]. Although an endogenous ligand for the sigma receptors remains unclear, some studies have reported that steroid hormones such as progesterone and testosterone might interact with sigma

receptors [4, 5]. Confirmed sigma$_1$ receptor ligand functions are neuro-protective, anti-depressant, and anti-amnestic functions [6, 7]. Sigma$_1$ receptor agonists improved impairment of learning and memory in mice [8–10]. Matsuno et al. [11–13] showed that the sigma$_1$ receptor agonists such as (+)-SKF-10,047 and SA4503 increased extracellular acetylcholine levels in the rat frontal cortex and hippocampus. The sigma$_1$ receptor is considered to be involved in aging [14, 15] and various diseases, such as schizophrenia [16], depression [17], ischemia [18], and Parkinson's disease [19]. In patients with Alzheimer's disease (AD), a postmortem study showed that the sigma$_1$ binding sites were reduced in the hippocampus [20]. The sigma$_1$ receptor agonists are also expected as drugs for improving the cognitive deficits of AD [21]. However, the distribution of sigma$_1$ receptors in patients with AD remains to be determined. We developed a positron emission tomography (PET) ligand, [^{11}C]SA4503 (Fig. 1), for mapping the sigma$_1$ receptors [22–24], and reported that sigma$_1$ receptor was down-regulated in the putamen with Parkinson's disease [19]. The objective of this study was to investigate the change of sigma$_1$ receptor in the early phase of AD using [^{11}C]SA4503 PET.

Materials and methods

Subjects

We studied five patients (two men and three women, mean age ± SD, 74.6 ± 3.2 years) diagnosed as having probable AD on the basis of the National Institute of Neurological and Communicative Diseases and Stroke/Alzheimer's Disease and Related Disorders Association (NINCDS–ADRDA) criteria [25]. Magnetic resonance imaging (MRI) scans were obtained with a MAGNEX 1.5-T machine (Shimadzu, Kyoto, Japan) in the First Hospital of Nippon Medical School, and we confirmed that they had no diseases other than AD including stroke and brain tumor. To ensure the early diagnosis of AD, each patient was also examined for glucose metabolism by PET using [^{18}F]fluorodeoxyglucose ([^{18}F]FDG), and we confirmed hypometabolism of glucose in the temporoparietal lobe and posterior cingulate of all patients [26, 27]. The clinical severity of AD was scored in each patient according to the Functional Assessment of Staging [28], Mini-Mental State examination [29], and Clinical Dementia Rating [30] just before the [^{18}F]FDG PET examination.

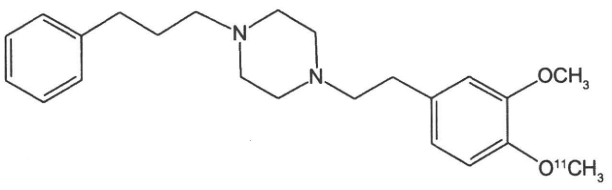

Fig. 1 Chemical structure of [^{11}C]SA4503

The control group consisted of seven volunteers (two men and four women, age ± SD 62.6 ± 8.2), without any history of neurological diseases or abnormalities on physical or neurological examinations. MRI scans were obtained with a SIGNA 1.5-T machine (General Electric, WI, USA) in the Tokyo Metropolitan Geriatric Hospital for the normal subjects, and we confirmed that they had no neurological diseases, such as stroke and brain tumor. They were not currently receiving medications known to affect brain metabolism. None had a history of alcoholism.

The Ethics Committee of Tokyo Metropolitan Institute of Gerontology approved this study protocol. Informed consent in writing was obtained from all of the subjects who participated in this study.

[^{11}C]SA4503 PET

Positron emission tomography was performed in the Tokyo Metropolitan Institute of Gerontology Positron Medical Center with an SET2400 W scanner (Shimadzu, Kyoto, Japan) [31]. [^{11}C]SA4503 was prepared as described earlier [23]. The specific activity at the time of injection ranged from 23.7 GBq/μmol to 130.2 GBq/μmol (72.3 ± 34.3 GBq/μmol). The transmission data were acquired with a rotating ^{68}Ga/^{68}Ge rod source for attenuation correction. A dynamic series of decay-corrected PET data acquisition was performed in the 2D mode for 90 min starting at the time of the injection of 500 MBq of [^{11}C]SA4503. Arterial blood was sampled at 10 s, 20 s, 30 s, 40 s, 50 s, 60 s, 70 s, 80 s, 90 s, 100 s, 110 s, 120 s, 135 s, and 150 s, and at 3 min, 5 min, 7 min, 10 min, 15 min, 20 min, 30 min, 40 min, 50 min, 60 min, 75 min, and 90 min. Plasma was separated, weighed, and measured for radioactivity with an NaI (Tl) well scintillation counter. Metabolite analysis was carried out by high-performance liquid chromatography [23].

Data analysis

Image manipulations were carried out on an O2 workstation (Silicon Graphics, Mountain View, CA, USA), using a medical image processing application package "Dr. View" version 5.2 (AJS, Tokyo, Japan).

For [^{11}C]SA4503 PET, we generated early images for each subject by adding up the frames of the dynamic scan from 0 min to 10 min [32]. Circular regions of interest (ROIs) 10 mm in diameter and extending over two slices of the images were drawn on the cerebellum, medial temporal lobe (included hippocampus), frontal lobe, temporal lobe, occipital lobe, parietal lobe, post cingulate gyrus, thalamus, and striatum. The time course of the tissue concentration of [^{11}C]SA4503 was computed from the PET data and the interpolated ROIs throughout the scanning period. A two-tissue three-compartment model was used to estimate K_1, k_2, k_3, k_4, and the delay between metabolite-corrected plasma and tissue time activity using a Gauss–Newton algorithm [15]. The ratio of k_3 to k_4 was computed as the binding potential (BP), which is linearly related to the density of sigma$_1$ receptors. Parametric images of total distribution volume (DVt) for [^{11}C]SA4503 were also generated using a graphical analysis [33].

Statistics

Unpaired t tests were used to compare the BP in patients with AD and normal subjects. The Bonferroni correction was applied for multiple comparisons (nine comparisons corresponding to nine regions). The level of significance was set at $P < 0.05$. The statistical computation was performed using a software package "JMP" version 5.1.2 (SAS Institute, Cary, NC, USA) on a Macintosh computer.

Results

Table 1 summarizes the clinical profiles. Their average duration of illness was 2.0 ± 0.7 years. The severity of cognitive dysfunction as assessed with the Mini-Mental State examination ranged from 16 to 25.

In the ROI-based analysis, K_1 for [^{11}C]SA4503 was significantly lower in the parietal lobe of the AD patients than in that of normals, whereas there was no significant difference in other regions between AD patients and the normals (Table 2). On the other hand, BP for [^{11}C]SA4503 was significantly lower in the frontal, temporal, and occipital lobes, cerebellum and thalamus of the AD patients than in that of normals (Table 2). We also observed that BP also showed a tendency to decline in other regions of AD. Figure 2 shows representative PET images for a normal subject and a patient with AD. The DVt image demonstrates that the sigma$_1$ receptors are lower in the entire brain of the patient with AD than in that of the normal subject.

Discussion

[^{11}C]SA4503 PET demonstrated that the distribution of cortical sigma$_1$ receptors was reduced in the early phase of AD. Only in the parietal lobe could we observe a significant reduction of K_1, which was linearly related to the cerebral blood flow. The age of the control subjects was slightly younger than that of the patient group. However,

Table 1 Demographic and clinical data for patients with Alzheimer's disease (AD)

No.	Age (years)	Sex	Duration (year)	Medication before PET	FAST	MMS	CDR
1	79	M	3	Donepezil	3	25	1
2	76	M	2	Donepezil	3	21	1
3	75	F	1	Donepezil	4	16	1
4	71	F	2	None	3	17	1
5	72	F	2	None	3	22	1

PET positron emission tomography, *FAST* functional assessment of staging, *MMS* Mini-Mental State examination, *CDR* clinical dementia rating

Table 2 Comparison of K_1 and binding potential for sigma$_1$ receptors in each region in normals and patients with AD

ROI	K_1		BP	
	Normal	AD	Normal	AD
Frontal lobe	0.50 ± 0.06	0.43 ± 0.06	16.4 ± 3.0	9.2 ± 4.5*
Temporal lobe	0.52 ± 0.07	0.44 ± 0.04	17.4 ± 3.6	8.7 ± 4.3*
Hippocampus	0.46 ± 0.06	0.42 ± 0.03	18.6 ± 3.8	12.2 ± 6.8
Occipital lobe	0.58 ± 0.07	0.50 ± 0.09	13.7 ± 2.6	5.9 ± 3.3**
Parietal lobe	0.52 ± 0.06	0.39 ± 0.06*	16.7 ± 2.6	13.6 ± 10.5
Posterior cingulate	0.62 ± 0.08	0.50 ± 0.09	15.4 ± 3.2	8.7 ± 5.4
Cerebellum	0.56 ± 0.10	0.58 ± 0.06	22.5 ± 4.8	9.0 ± 5.1**
Striatum	0.55 ± 0.07	0.57 ± 0.07	13.9 ± 2.4	8.8 ± 3.5
Thalamus	0.64 ± 0.09	0.62 ± 0.09	15.2 ± 4.7	6.9 ± 2.3*

ROI regions of interest, *BP* binding potential, *AD* Alzheimer's disease
Values are mean ± SD (normal $n = 7$, AD $n = 5$).
*$P < 0.05$, **$P < 0.01$ (unpaired t test)